Acta Radiologica Open
7(6) 1–8

DOI: 10.1177/2058460118783013
journals.sagepub.com/home/arr
SAGE

Diffusion-weighted imaging in acute pulmonary embolism: a feasibility study

Roberto Vargas Paris[1,2], Mikael Skorpil[3,4], Eli Westerlund[5,6], Peter Lindholm[1,7] and Sven Nyrén[3,7]

Abstract

Background: Magnetic resonance imaging (MRI) can be an alternative method to computed tomography angiography (CTA) for pulmonary embolism.

Purpose: To evaluate the feasibility of diffusion-weighted imaging (DWI) detecting acute pulmonary embolism (PE) in free-breathing humans.

Material and Methods: Twenty patients with PE verified by CTA and 20 controls were investigated with MRI (1.5 Aera, Siemens Healthcare). All sequences were performed in the transversal plane using free-breathing without gating. The protocol consisted of a two-dimensional steady-state free precession (SSFP) and a single-shot DWI echo-planar imaging sequence with a voxel resolution of $2 \times 2 \times 5$ mm. Three b values were used: 50, 400, and 800 s/mm^2. Images were analyzed in two orders: an open source analysis (OSA); and a blinded only DWI analysis (BDA) simulating clinical work.

Results: OSA of corresponding images showed 370 findings on CTA (i.e. one elongated emboli could be represented in multiple images). SSFP identified 237 of those (64%). DWI with b values of 50, 400, and 800 identified 327 (88%), 245 (66%), and 138 (37%), respectively. In BDA we found 160 true emboli (according to CTA) on b50, 78 on b400, and 54 on b800. Fifty-two of these findings at the subsegmental level could be correlated to PE on CTA but were not visible on SSFP.

Conclusions: DWI has a high sensitivity for detecting PE but suffers from poor specificity. It could potentially be used as an eye catcher, i.e. where to look for PE in other MRI sequences.

Keywords
Magnetic resonance imaging, lung, pulmonary embolism, human

Date received: 13 February 2018; accepted: 19 May 2018

Introduction

Diffusion-weighted imaging (DWI) is currently increasingly being utilized in clinical practice: for example, in differentiating benign from malignant tumors (1), detecting ischemic brain lesions (2), abdominal nodal staging (3), and evaluating peripheral nerves (4). DWI is a magnetic resonance imaging (MRI) technique quantifying the motion of water protons and is acquired by applying strong motion encoding gradients. The b value encodes the amount of diffusion and the apparent diffusion coefficient (ADC) quantifies it (5).

Pulmonary embolism (PE) is a potentially life-threatening disease that should be diagnosed quickly. Autopsy studies have shown that approximately 10% of hospital deaths are caused by PE (6). The current

[1]Department of Physiology and Pharmacology, Karolinska Institutet, Stockholm, Sweden
[2]Abdominal Radiology, Imaging and Physiology, Karolinska University Hospital, Stockholm, Sweden
[3]Department of Molecular Medicine and Surgery, Karolinska Institutet, Karolinska University Hospital, Stockholm, Sweden
[4]Department of Neuroradiology, Karolinska University Hospital, Stockholm, Sweden
[5]Department of Clinical Sciences, Karolinska Institutet, Danderyd Hospital, Stockholm, Sweden
[6]Division of Medicine, Danderyd Hospital, Stockholm, Sweden
[7]Thoracic Radiology, Imaging and Physiology, Karolinska University Hospital, Stockholm, Sweden

Corresponding author:
Roberto Vargas Paris, Abdominal Radiology, A1:01, MRI Department, Karolinska University Hospital, SE-171 76 Stockholm, Sweden.
Email: roberto.vargas@ki.se

standard radiological examination is computed tomography angiography (CTA). MRI is an alternative method for diagnosing PE, where various sequences have been evaluated, such as steady-state free precession (SSFP) and angiography with gadolinium contrast media. MRI generally shows high specificity but low sensitivity in detecting PE (7,8), suggesting that new approaches or added features are needed to improve sensitivity.

Today the role of MRI in detecting PE is not well defined, the access to the method is limited, and it has not yet evolved as a clinical method. MRI could be of great benefit, since CTA cannot be used in patients with renal dysfunction; additionally, MRI has the advantage of not using ionizing radiation (9). A robust non-contrast-enhanced MRI protocol could prove to be an alternative in patients with contraindications to iodine contrast agencies or a younger population (10).

MRI has limitations in pulmonary diseases, due to the low proton density of lung parenchyma and susceptibility artifacts at the interface between air and lung tissue (11). Motion artifacts from the beating heart and breathing further reduce image quality. Despite these limitations, MRI is valuable for thoracic imaging and new applications are being developed. Furthermore, no previous study has investigated the possibility to detect acute PE in humans and very few studies have been performed using DWI in thrombosis detection. A study in mice (12) induced experimental venous thrombi in the inferior vena cava and demonstrated the possibility to detect these with DWI, as well as to follow diffusion changes during the degradation of thrombi. In a study on humans from Catalano et al. (13), DWI could distinguish malignant from bland portal vein thrombi in patients with hepatocellular carcinoma. We therefore hypothesized that PE could be differentiated from flowing pulmonary blood using DWI, and that it would identify PE in patients during free-breathing acquisition.

The aim of this study was to evaluate the feasibility of DWI detecting acute PE in free-breathing humans and assess ADC values in PE.

Material and Methods

The study was performed according to the Helsinki Declaration and was approved by the local institutional review board. Written informed consent was obtained from each patient and volunteer.

Participants

A total of 20 patient with PE verified on CTA (64-slice CT scanner, Lightspeed VCT, General Electric Medical Systems, Milwaukee, WI, USA; Ultravist 370 mg I/mL, Bayer HealthCare Pharmaceuticals Inc., Berlin, Germany), slice thickness was 0.63 mm and reconstructed into 2-mm and 5-mm slices. All the patients were in-house and recruited between May 2012 and November 2013, from the Emergency Department. The patients were included based on availability of the MRI scanner and if the clinician involved in the study was in service. Only patients that were unstable or with contraindications to MRI were excluded. No patient declined the invitation. All were investigated with MRI within 48 h (mean = 26 h; range = 3.5–47 h). The group consisted of 16 men (mean age = 59 years; age range = 24–88 years) and four women (mean age = 57 years; age range = 24–85 years). All patients were under treatment based on the CTA findings before participating in the study protocol with MRI. As a reference group, 20 healthy volunteers were recruited and investigated with MRI only (no CTA). This group had neither history of PE nor any hospital records of PE six months after MRI. The control group consisted of four men (mean age = 43 years; age range = 27–67 years) and 16 women (mean age 45 years; age range = 27–64 years).

MRI protocol

All 40 participants (20 patients and 20 volunteers) were examined on a 1.5-T MRI scanner (Aera, Siemens Healthcare, Erlangen Germany) with an 18-channel body matrix coil and a spine matrix coil. All were instructed to breathe normally during the sequences. Neither ECG nor respiratory gating was used. The protocol consisted of a two-dimensional true FISP fast imaging with a steady-state precession gradient echo (SSFP) sequence in the transversal plane covering the entire lung artery territory: TR/TE = 3.6/1.3 ms; voxel resolution = $0.9 \times 0.9 \times 4.5$ mm; slices = 90, and number of excitations (NEX) = 1. Next, a single-shot DW echo-planar imaging (EPI) sequence was performed in the transverse plane: TR/TE = 5600/60 ms; in-plane voxel resolution = $2 \times 2 \times 5$ mm; NEX = 4. Three b values were used: 50, 400, and 800 s/mm^2. IPat® = 2 and SPAIR for fat saturation was used. ADC maps were automatically generated by the scanner using all three b values. Total scanning time was approximately 20 min.

Image evaluation

Open source analysis (OSA). MRI images were evaluated in the Picture Archive and Communication System (PACS) in consensus by a senior thoracic radiologist (SN) and a senior MRI radiographer (RVP), both had > 20 years of experience in their field including

thoracic radiology and MRI. They evaluated the corresponding images for DWI, SSFP, and CTA. In this analysis, corresponding images for an anatomical location, were compared, i.e. the number of findings could be larger than the actual number of emboli, since an embolus could stretch through many slices if elongated. PEs were also classified according to vascular territories as central, lobar, segmental, or subsegmental.

The patient group in OSA analysis (both MRI and CTA). The radiologist compared the locations of PE in CTA with areas of restricted diffusion in DWI; in other words, in areas with high signal intensities, which was not always present in all three different b value images. Due to the poor anatomical information in DWI, we used a crosshair tool in the PACS, to correlate the position of the high signal intensity in DWI with anatomy provided by the SSFP sequence. Restricted diffusion signal intensities presented in DWI images that were not correlated to a PE were classified as lymph nodes, pleural fluid, or lung consolidation, using both the SSFP and the CTA as reference. Regarding artifacts like distortion, they were not considered as a problem to be confused with PE and were not included in the analysis. When high DWI signal intensities were present in all three b value images, a region of interest (ROI) was marked by the radiographer, yielding an ADC value. ROIs were circular, at least 5 mm in diameter, and carefully placed in the center of the signal area in the ADC map avoiding lung tissue. A regression analysis of the ADC values of the thrombi versus the time between CTA and MRI was performed.

The volunteer group in the OSA analysis (SSFP and DWI only). The high signal intensities detected in DWI images were compared with the anatomical SSFP. The high signal intensity was classified by the radiologist as a possible PE (= false positive) when located intravascularly in the pulmonary artery; otherwise they were classified as lymph node or other abnormality. Node maps proposed from the International Association for the Study of Lung Cancer were used (14). ADC values were calculated when signal was present in all three b value images.

Blinded DWI analysis (BDA) with only the patients group included. In an alternative analysis made > 1 year after the OSA, only the DWI from the patient group were reviewed separately by two blinded radiologists (both with > 20 years of experience; SN, MÖ). Neither the CTA nor the SSFP images were available for anatomical or pathological correlation. One patient had no pulmonary emboli detected on the CTA and was therefore later excluded from the study. Thus, 19 individuals remained. DWI findings were numbered, noted, and drawn in a standard anatomical image (sheet), and the slice and the anatomical position recorded by each observer independently. Every finding was classified as a vessel or lymph node. The anatomical level was noted (subsegmental, segment, lobar, or central) and if the finding were seen in one, two, or three b values. As the numbering and anatomical grouping of the DWI findings differed between the two observers, the findings had to be regrouped into a matrix, e.g. a diffuse finding of one segmental DWI finding by one radiologist could have been marked as two subsegmental findings by the other, etc. This was performed at a later stage by one of the observers (SN) with corresponding access to CT and SSFP images for anatomical positioning. Every DWI finding noted by either of the observers was entered to the matrix and correlated with the same DWI finding of the other observer, when possible, and confirmed by CTA. The noted slice position and the schematic drawing in the anatomical sheet were used to ensure that the findings described were the same. In this matrix, if the findings were correlated with a thrombus seen in the CTA, then they were classified as a true finding. It was sometimes noted by both observers, but if not, it was classified as missed by one of the observers. Occasionally a DWI finding had no correlating thrombus on the CTA and was classified as false positive. At the same time, all the DWI findings were correlated to the SSFP sequence if the thrombus was or was not seen there.

In this analysis, the radiologists rated the number of emboli, i.e. not the number of findings in each slice, simulating the clinical way of working, but limited to only DWI images. Descriptive statistics are presented as mean ± 1 standard deviation and range. The two-tailed Student's t-test (Excel, 2007) was used for significance testing; $P < 0.05$ was considered significant.

Results

OSA: All 20 patients and 20 volunteers completed the protocol and no images were excluded. In the patient group, a total of 370 findings were detected by CTA (Figs. 1–3 and Table 1). Note that "finding" here represents a finding in one transversal image plane, not one emboli since emboli may be elongated and appear in multiple images. SSFP identified 237 of those (64%). DWI with b values of 50, 400, and 800 identified 327 (88%), 245 (66%), and 138 (37%), respectively. In the healthy group, high DWI signal intensities were detected in 186 locations for b = 50, of which 120 could be anatomically identified as lymph nodes. Thus, in 66 locations within the lung artery territory among the healthy individuals, no PE or other abnormalities were found (66 in b = 50, 29 in b = 400, and 13 in b = 800, respectively). These 66 high signal intensities

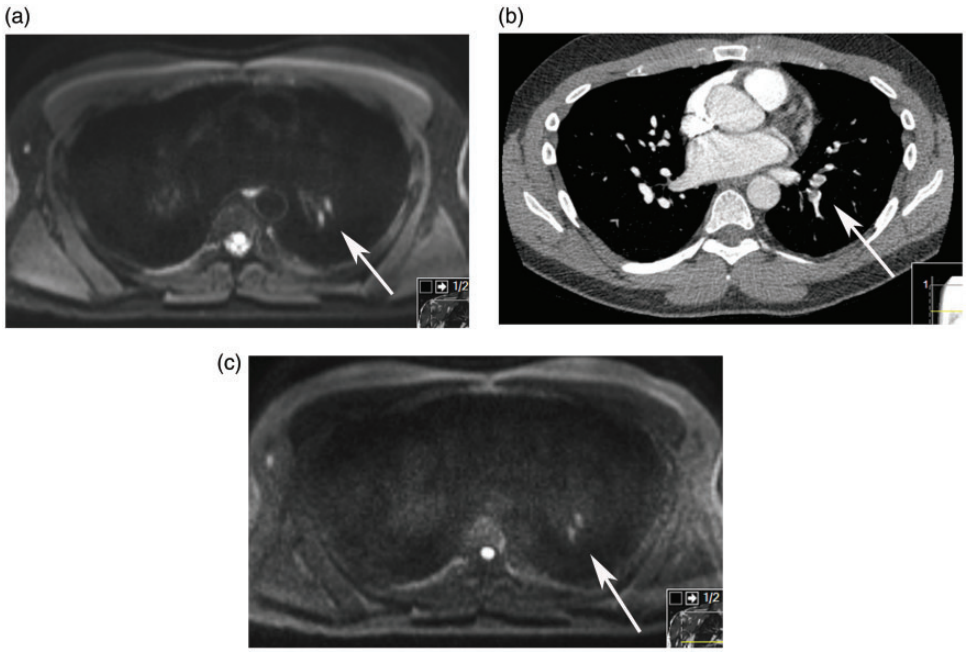

Fig. 1. (a) DWI with b value of 50 s/mm^2; (b) CTA; and (c) DWI with b value of 800 s/mm^2. Two PEs were identified in the left lower lobe at the segmental level, in all the three sequences (indicated by white arrow).

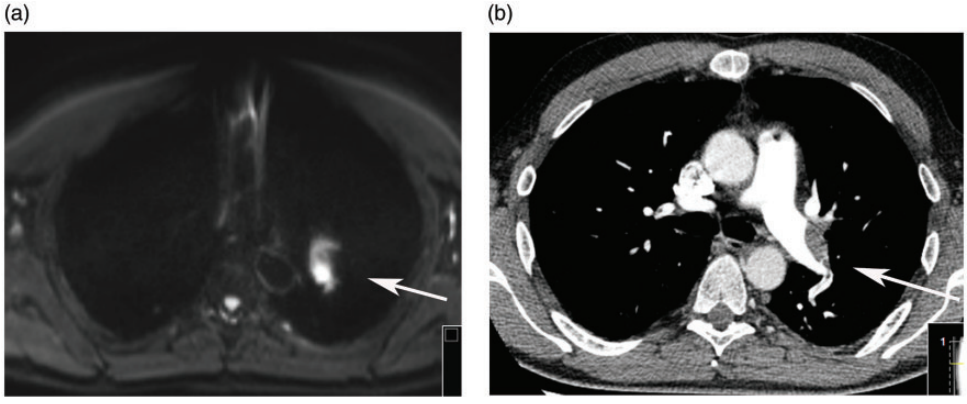

Fig. 2. (a) DWI with b values of 50 s/mm^2 and (b) CTA. Large central PE was identified in the left pulmonary artery (white arrow).

were classified as false positive. While in the patient group, false positives were identified in 22, seven, and three areas in b = 50, b = 400, and b = 800, respectively.

Our results showed that DWI detected a larger number of emboli compared to transverse SSFP. Many of the patients had multiple emboli seen in multiple slices (note that the total of 370 in OSA represents individual findings in corresponding images, not the number of emboli, since a single emboli could be elongated and stretch through many slices/transverse images, in 20 patients), but if we classify each participant as having or not having high signal intensities within the pulmonary artery territory, we can calculate an overall sensitivity and specificity for making a PE diagnosis (Table 2). DWI then has a sensitivity of 100%, 95%, and 90% for b = 50, b = 400, and b = 800, respectively. Using our healthy group as true negatives, DWI has a specificity of 15%, 40%, and 60% for b = 50, b = 400, and b = 800, respectively.

PEs were also classified according to vascular territories as central, lobar, segmental, or subsegmental (Table 1). Some central emboli could not be detected in all b values, while b = 50 still detected most emboli on the segmental and subsegmental level.

We measured the ADC of the pulmonary emboli; a total of 138 emboli were distinguishable to be

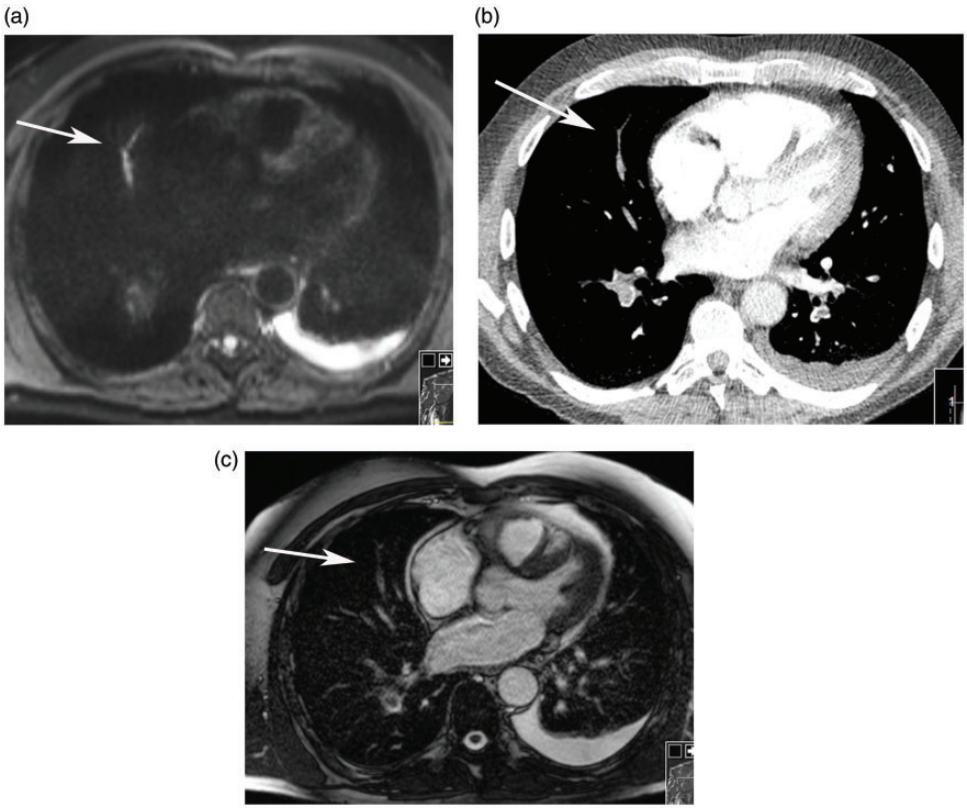

Fig. 3. (a) DWI b value of 50 s/mm^2, respectively; (b) CTA shows two subsegmental emboli; and (c) SSFP does not clearly show a PE. Note that PEs were clearly visible and probably identified more quickly with the DWI images (white arrows).

Table 1. Anatomical location of PE findings.

Anatomic position	Total PE				
	CTA	SSFP	DWI 50	DWI 400	DWI 800
Central	36	35 (97)	33 (91)	29 (80)	21 (58)
Lobar	80	74 (92)	76 (95)	68 (85)	46 (57)
Segmental	113	88 (77)	99 (87)	69 (61)	38 (33)
Subsegmental	141	40 (28)	119 (84)	79 (56)	33 (23)

Values are shown as n (%) of PEs found on CTA that were identified with SSFP and three levels of diffusion encoding (b = 50, 400, 800) according to the pulmonary vasculature anatomy.

Table 2. Correlation between CTA/DWI findings.

	b = 50		b = 800	
Threshold	CTA+	CTA–	CTA+	CTA–
DWI+	20	17	18	8
DWI–	0	3	2	12

In this study, the healthy controls are designated CTA– and the patients with PE, CTA+. The table shows the number of patients with PE that were identified (CTA+, DWI+) or not identified (CTA+, DWI–) at two given b values. Additionally, the number of healthy individuals with DWI findings indicating PE, but not having PE, (CTA–, DWI+) or truly identified as not having PE (CTA–, DWI–) are seen.

measured with a 5-mm ROI. This required identification in all b values and data were divided into two anatomical levels: subsegmental–segmental and lobar–central (Table 3). We also measured ADC in lymph nodes in the volunteer group (only in volunteers to avoid a possible pathological nodule) (Table 3). To confirm that our method and ADC values were reasonable we also measured ADC in two tumors (0.5 and 1.1×10^{-3}mm^2/s, respectively) and three cases with pleural fluid (a mean of 3.2×10^{-3}mm^2/s). We did not make a full evaluation of every other condition, but tumor and pleural fluid had different ADCs, while lymph nodes and lung consolidation had similar values to PEs (Table 3) (no significant differences). As the numbers of tumor/fluid were small, no statistical evaluation was made.

The *P* value of the ADC thrombi vs. the time between CTA and MRI was 0,7, thus not significant.

BDA: Altogether 204 DWI findings were noted by any of the observers. Note that "finding" in this analysis represents a finding sometimes stretching through

multiple imaged planes in the transverse sections possibly representing one emboli each, separating this analysis from the exact correlation of CTA vs. SSFP under OSA where there were 370 "findings." When the 204 DWI findings were correlated with the SSFP and CTA images, 34 of these were shown to be related to lymph nodes. Three of these were in the lobar or segmental levels, the rest in the central level. Observer 1 noted 27 and observer 2 noted 23 of these. Fifteen findings were noted by both. Observer 1 misinterpreted 22 and observer 2 misinterpreted 13 of these as related to vessels.

Of the remaining 170 findings, ten were not related to vessels, of which four had no anatomic correlation at all. One represented the lower end of a tumor falsely interpreted as a vessel finding by observer 2. Observer 1 noted three and observer 2 four DWI findings that had no correlation to thrombi in vessels (one in common), thus there were six false positive findings, including the tumor. The remaining 160 DWI findings represented thrombi in vessels, where 160 were seen on b = 50, 78 on b = 400, and 54 on b = 800.

Table 3. ADC values by pathology and anatomic position.

Position	Measurements (n)	Mean ADC (SD) (mm^2/s)
Central/Lobar PE	70	$1.6\ (\pm 0.3) \times 10^{-3}$
Segment/Subsegment PE	68	$1.3\ (\pm 0.3) \times 10^{-3}$
Lymph nodes	50	$1.7\ (\pm 0.3) \times 10^{-3}$
Consolidation	13	$1.5\ (\pm 0.3) \times 10^{-3}$
Pleural fluid	3	$3.6\ (\pm 0.3) \times 10^{-3}$
Tumor	2	$0.78\ (\pm 0.3) \times 10^{-3}$
Total overall PE above (70 + 68)	138	$1.4\ (\pm 0.3) \times 10^{-3}$

ADC values from various findings in the MRI examinations with mean and standard deviation (SD). Not all findings were shaped appropriately for ROI measurements; thus, for example, the number of emboli are slightly fewer than in Table 1, b = 800.

Of special interest is that 68 out of 160 of the DWI findings that correlated with thrombi were detected on CTA but were not seen on the SSFP. Of these, 52 were on the subsegmental level (seven segmental, six lobar, and three central). Of the corresponding findings that were seen in both SSFP and CTA, the location was 21 subsegmental, 27 segmental, 30 lobar, and 14 central.

Discussion

The principal finding in this study was that diffusion-weighted MRI visualized PE in patients without gating or breath-hold. The method suffers from poor specificity, but could potentially be used as an eye catcher, i.e. where to look for PE in other MRI sequences.

The larger number of PE seen in b = 50, compared to b = 400 and b = 800, could be due to a T2 shining through effect.

The sensitivity to detect emboli was high in all b values, 90–100%, while the specificity was as low as 15% for b = 50 and best at 60% for b = 800 (Table 2). If we compare the capability of DWI to detect PE in a subsegmental level (Fig. 3), our study showed 84% for b = 50. Kluge et al. (15) presented sensitivities of 55% and 93% for MR angiography and MR perfusion, respectively, at the same anatomic level. Especially on a subsegmental level, DWI was better than SSFP. The DWI probably has no potential as a stand-alone method for the detection of PE but could add to the detection rate if combined with other imaging sequences.

The ADC values found for PE (Table 3) had a mean of $1.4 \times 10^{-3}\,mm^2/s$, with a range of 0.6–$2.5 \times 10^{-3}\,mm^2/s$. There are no published in vivo data from humans, but ex vivo data from Vidmar et al. (16) showed ADC values of 0.31 and $0.74 \times 10^{-3}\,mm^2/s$ for acute and chronic PE, respectively. Phinikaridou et al. published a study (12) where deep vein thrombi were induced in the inferior vena cavae of mice. Measurements on days 1, 7, 14, 21, and 28 after

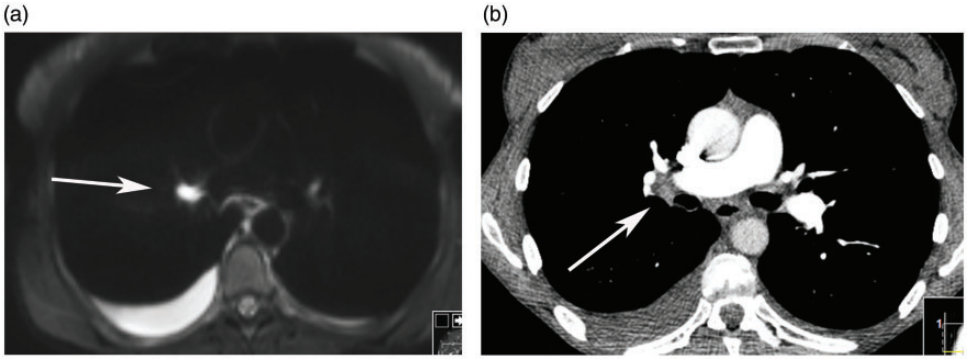

Fig. 4. (a) DWI with b values of 50; and (b) CTA. A typical hilar lymph node was shown in position R10.

thrombosis were made. The earliest and the oldest thrombotic processes had the lowest ADC values, 0.72 and 0.69, respectively, with the highest at day 14, with 1.1×10^{-3} mm^2/s. In 2012, Ichiki et al. (17) induced thrombi in the inferior vena cavae in pigs. Their mean ADC values after 2 h were 1.92×10^{-3} mm^2/s, at day 1 1.62×10^{-3} mm^2/s, and at day 3 1.67×10^{-3} mm^2/s. These data are comparable to ours of 1.4×10^{-3} mm^2/s.

Lymph nodes (Fig. 4) were also a common finding in our study, located mostly in the central lung parenchyma and mediastinal area. The mean ADC value obtained in lymph nodes of 1.7×10^{-3} mm^2/s is similar to benign nodes as shown by Kosucu et al. (18), which had ADC values of 1.0 in malignant and 1.5×10^{-3} mm^2/s in benign lymph nodes. The ADC values of lymph nodes and PE were similar in the lobar/central emboli where the whole emboli could be included in the ROI. ADC measurements (Table 3) of subsegmental/segmental emboli sometimes included tissue beyond the suspected emboli (due to the 5-mm ROI), and those values were slightly lower, most likely due to the limitations of accuracy in the measurements (Table 3). The measurements of tumors and pleural fluid confirmed a separate range. We did not measure or compare with other findings than emboli-healthy lymph nodes. Interestingly our findings suggest that emboli have similar ADC values as healthy lymph nodes.

MRI of the lungs suffers from a poor proton density causing low signal-to-noise ratio and is sensitive to distortion artifacts because of the large interface between air and parenchyma (11). The lungs move due to breathing, mechanical forces of the beating heart, and pulsatile blood flow. Movement artifacts have been shown to induce inaccuracies in ADC measurements (19). Individuals were breathing freely during all acquisitions without respiratory or cardiac gating. Cardiac and lung motion are well-known sources of artifacts (19,20), as well as pulsations from the aorta (21). Our study showed that it was possible to identify emboli, as well as measure ADC information of the PE from central to subsegmental levels, even though the patients were breathing freely and without any gating of data collection.

There were DWI findings that correlated with thrombi detected on CTA but were not seen on the SSFP. This could be due to artifacts or poor image quality in SSFP. Another interesting possibility is that DWI high signal is due to a reaction in the vessel wall lingering after the thrombus have moved or dissolved, and that this is not seen in SSFP. The number of emboli findings observed on the blinded analysis, on DWI and CT, but not SSFP, were highest for subsegmental emboli, 52 of the 68 emboli not seen with SSFP, which corresponds to the ones most hard to detect with SSFP, as well as the most likely to be dissolved (Fig. 3).

This adds into the limitation in our study, as with most studies on MRI and PE, which is the time lapse between the CTA and MRI examinations in the range of 3.5–47 h. Emboli verified on CTA might have dissolved partially or migrated, thus reducing sensitivity and specificity in our analysis. Almost all our patients were receiving anticoagulant treatment. We speculate that the ADC of acute PE in humans could be affected both by age of the emboli and therapeutic effect. Catalano et al. (13) discussed whether thrombi vascularity could affect the signal in DWI. Differences could also depend on different b values in various studies (as well as human vs. animals); Vidmar et al. (16) used 0, 260, 620; Phinikaridou et al. (12) used 0, 333, 667, and 1000; and Ichiki et al. (17) used 0 and 400 s/mm^2. Time and treatment might dissolve the thrombi giving less limited diffusion and higher ADC values, but our ADC values showed no major difference between 3.5 h and 46 h. This corresponds to the aim to evaluate the feasibility of using DWI together with other sequences, and not to evaluate or prove any clinical potential at this point. A further limitation was the lack of non-PE patients. We used volunteers and assumed that all were non-PE in the group without CTA from the observation that all were healthy on follow-up.

What we have interpreted as a DWI effect for the b value of 50 might be a T2 shining through effect rather than restricted diffusion.

In conclusion, DWI had a high sensitivity, but also false positive findings. DWI could potentially be helpful as an eye catcher in identifying arteries that should be studied more carefully (Figs. 1–3), possibly increasing quality, especially on a subsegmental level, and/or reducing reading time. DWI is increasingly used in the body to evaluate malignancy (21–24) and since PE is a common diagnosis in cancer patients, knowledge about the characteristics of PE could avoid a potential pitfall in clinical reading. The finding that DWI can detect PE during free-breathing could be especially important in patients who are in respiratory distress.

Declaration of conflicting interests

The author(s) declared no potential conflicts of interest with respect to the research, authorship, and/or publication of this article.

Funding

The author(s) disclosed receipt of the following financial support for the research, authorship, and/or publication of this article: This work was supported by the Swedish Heart and Lung Foundation, the Swedish Society of Medicine and Stockholm City Council.

ORCID iD

Roberto Vargas Paris http://orcid.org/0000-0002-7322-8546.

References

1. Colagrande S, Carbone SF, Carusi LM, et al. Magnetic resonance diffusion-weighted imaging: extraneurological applications. Radiol Med 2006;111:392–419.
2. van Everdingen KJ, van der Grond J, Kappelle LJ, et al. Diffusion-weighted magnetic resonance imaging in acute stroke. Stroke 1998;29:1783–1790.
3. Donati OF, Chong D, Nanz D, et al. Diffusion-weighted MR imaging of upper abdominal organs: field strength and intervendor variability of apparent diffusion coefficients. Radiology 2014;270:454–463.
4. Skorpil M, Engström M, Nordell A. Diffusion-direction-dependent imaging: a novel MRI approach for peripheral nerve imaging. Magn Reson Imaging 2007;25:406–411.
5. Hoeks CM, Barentsz JO, Hambrock T, et al. Prostate cancer: multiparametric MR imaging for detection, localization, and staging. Radiology 2011;261:46–66.
6. Kluetz PG, White CS. Acute pulmonary embolism: imaging in the emergency department. Radiol Clin North Am 2006;44:259–271.
7. Stein PD, Chenevert TL, Fowler SE, et al. Gadolinium-enhanced magnetic resonance angiography for pulmonary embolism (PIOPED III). Ann Intern Med 2010;152:434–443.
8. Revel MP, Sanches O, Lefort C, et al. Diagnostic accuracy of unenhanced, contrast-enhanced perfusion and angiographic MRI sequences for pulmonary embolism diagnosis: results of independent sequence readings. Eur Radiol 2013;23:2374–2382.
9. Araoz PA, Haramati LB, Mayo JR, et al. Panel discussion: pulmonary embolism imaging and outcomes. Am J Roentgenol 2012;198:1313–1319.
10. Ohno Y, Yoshikawa T, Kishida Y, et al. Unenhanced and contrast-enhanced MR angiography and perfusion imaging for suspect pulmonary thromboembolism. Am J Roentgenol 2017;208:517–530.
11. Biederer J, Mirsadraee S, Beer M, et al. MRI of the lung (3/3)-current applications and future perspectives. Insights Imaging 2012;3:373–386.
12. Phinikaridou A, Andia ME, Saha P, et al. In vivo magnetization transfer and diffusion-weighted magnetic resonance imaging detects thrombus composition in a mouse model of deep vein thrombosis. Circ Cardiovasc Imaging 2013;6:433–440.
13. Catalano OA, Choy G, Zhu A, et al. Differentiation of malignant thrombus from bland thrombus of the portal vein in patients with hepatocellular carcinoma: application of diffusion-weighted MR imaging. Radiology 2010;254:154–162.
14. Rusch V, Asamura H, Watanabe H, et al. The IASLC lung cancer project: a proposal for a new international lymph node map in the forthcoming seventh edition of the TNM classification for lung cancer. J Thorac Oncol 2009;4:568–577.
15. Kluge A, Luboldt W, Bachmann G. Acute pulmonary embolism to the subsegment level: diagnostic accuracy of three MRI techniques compared with 16-MDCT. Am J Roentgenol 2006;187:7–14.
16. Vidmar J, Kralj E, Bajd F, et al. Multiparametric MRI in characterizing venous thrombi and pulmonary thromboemboli acquired from patients with pulmonary embolism. J Magn Reson Imaging 2015;42:354–361.
17. Ichiki M, Sakai Y, Nango M, et al. Experimental venous thrombi: MRI characteristics with histopathological correlation. Br J Radiol 2012;85:331–338.
18. Koşucu P, Tekinbaş C, Erol M, et al. Mediastinal lymph-nodes: assessment with diffusion-weighted MR imaging. J Magn Reson Imaging 2009;30:292–297.
19. Le Bihan D, Poupon C, Amadon A, et al. Artifacts and pitfalls in diffusion MRI. J Magn Reson Imaging 2006;24:478–488.
20. Van Beek E, Wild J, Fink C, et al. MRI for the diagnosis of pulmonary embolism. J Magn Reson Imaging 2003;18:627–640.
21. Koh DO, Takahara T, Imai Y, et al. Practical aspects of assessing tumors using clinical diffusion-weighted imaging in the body. Magn Reson Med Sci 2007;6:211–224.
22. Nasu K, Kuroki Y, Nawano S, et al. Hepatic metastases: diffusion-weighted sensitivity-encoding versus SPIO-enhanced MR imaging. Radiology 2006;239:122–130.
23. Koh DO, Collins DJ, Orton MR. Intravoxel incoherent motion in body diffusion-weighted MRI: reality and challenges. Am J Roentgenol 2011;196:1351–1361.
24. Barral M, Taouli B, Guiu B, et al. Diffusion-weighted MR imaging of the pancreas: current status and recommendations. Radiology 2015;274:45–63.